ACS APPLIED MATERIALS & INTERFACES

Letter

www.acsami.org

Matching Solid-State to Solution-Phase Photoluminescence for Near-Unity Down-Conversion Efficiency Using Giant Quantum Dots

Christina J. Hanson,[†] Matthew R. Buck,[†] Krishna Acharya,[†] Joseph A. Torres,[‡] Janardan Kundu,[†] Xuedan Ma,[†] Sarah Bouquin,[†] Christopher E. Hamilton,[‡] Han Htoon,[†] and Jennifer A. Hollingsworth*[,†]

[†]Materials Physics and Applications Division: Center for Integrated Nanotechnologies and [‡]Materials Science and Technology Division: Polymers & Coatings, Los Alamos National Laboratory, Los Alamos, New Mexico 87545, United States

Supporting Information

ABSTRACT: Efficient, stable, and narrowband red-emitting fluorophores are needed as down-conversion materials for next-generation solid-state lighting that is both efficient and of high color quality. Semiconductor quantum dots (QDs) are nearly ideal color-shifting phosphors, but solution-phase efficiencies have not traditionally extended to the solid-state, with losses from both intrinsic and environmental effects. Here, we assess the impacts of temperature and flux on QD phosphor performance. By controlling QD core/shell structure, we realize near-unity down-conversion efficiency and enhanced operational stability. Furthermore, we show that a simple modification of the phosphor-coated light-emitting diode device—incorporation of a thin spacer layer—can afford reduced thermal or photon-flux quenching at high driving currents (>200 mA).

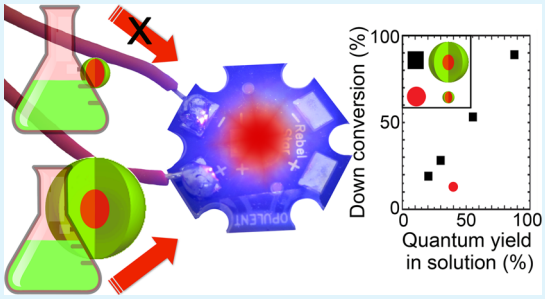

KEYWORDS: *giant quantum dots, down-conversion materials, high power light-emitting diodes, solid-state lighting*

Development of solid-state lighting (SSL) for domestic and commercial use is driven by the current high energy costs associated with conventional lighting, i.e., ∼20% of all energy consumption.[1] SSL relies on semiconductor light-emitting diodes (LEDs), which generate light as a result of electron−hole recombination at the p−n junction of the diode. Most current commercial LEDs produced for domestic white-light generation depend on partially down-converting a blue LED with a broadband yellow phosphor, with the resulting mixture of blue and yellow giving the appearance of white light. This choice of excitation LED and phosphor has largely been dictated by the availability of both efficient blue LEDs and an efficient and stable yellow phosphor, namely, cerium(III) doped yttrium aluminum garnet (YAG:Ce^{3+}).[2] However, although YAG:Ce^{3+} is renowned for its high quantum yield in emission (QY) and insensitivity to flux-density saturation (exhibits linear increase in emission intensity with increasing excitation intensity), its spectral full-width-at-half-maximum (fwhm) (∼80−100 nm) is not ideal for newer LED design concepts that are based on creating high-quality white light from a suitable collection of narrowband emitters,[3] and alone it is incapable of providing an ideal color-rendering index (CRI) or "warm-white" color temperatures.[4,5] Inclusion of a red-emitting phosphor would enable the YAG:Ce^{3+}-altered blue LED to achieve high CRI values and tunable color temperatures by filling the red spectral gap.[6]

The key technical challenge for this approach (or alternatives that rely on combining green and red phosphors) is the lack of a narrowband, efficient and robust red-emitting phosphor. Existing red phosphors that are sufficiently efficient and stable are broadband (fwhm: >100 nm), e.g., the commercial nitride red phosphor, $Sr_2Si_5N_8$:Eu^{2+},[7] such that much of the "red" emission lies outside the spectral region detected efficiently by the human eye, resulting in a poor luminous efficacy of radiation (LER). Trivalent rare earth emitters, such as Y_2O_3:Eu^{3+} and Y_2O_2S:Eu^{3+}, are "line emitters" that can provide the desired color quality; however, these phosphors lack broadband and efficient excitation pathways in the UV/blue (relying on formally electric dipole forbidden optical transitions). Trivalent rare earth emitters are also challenged by long radiative decay times (rapid flux saturation), low emission efficiencies, chemical/thermal instabilities (sulfide and oxysulfide hosts), and/or costly syntheses (e.g., nitride hosts synthesized above 1000 °C using high nitrogen pressures).[2] In addition to technical limitations, socio-economic factors are driving appeals for minimizing rare earth components in commercial products to reduce vulnerabilities to both near- and longer-term supply disruptions.

For these reasons, new narrowband red down-converter materials are needed that address existing technical limitations but also do not rely on rare-earth emitters. Semiconductor quantum dots (QDs) are potential alternative down-converter materials for lighting. As excitonic (bandgap) emitters, they are inherently capable of narrowband emission (fwhm: 25−35 nm) that is accompanied by efficient, broadband absorption for facile excitation. Indeed, high CRI values have been

Received: March 31, 2015
Accepted: June 8, 2015
Published: June 8, 2015

DOI: 10.1021/acsami.5b02818
ACS Appl. Mater. Interfaces 2015, 7, 13125−13130

demonstrated for white-light LEDs combining YAG:Ce^{3+} and red-emitting QDs.[6,8,9]

Despite many promising attributes, QDs are themselves challenged by several key features that limit their potential as rare-earth-phosphor alternatives. It is well-known that QDs can be synthesized to have near-unity solution-phase QYs either by coating the emissive QD core with a protective layer of organic surfactant ("ligand") molecules or an inorganic (wider bandgap semiconductor) shell.[10,11] However, neither the organic ligands nor the inorganic shell keeps the QDs from succumbing to unwanted "dark" processes—fluorescence intermittency (blinking), photobleaching, solid-state/environmental quenching, nonradiative Auger recombination. These processes, along with QD-QD energy transfer activated in densely packed QD films,[12] turn solution-phase 100% QYs into solid-state 1−10% QYs. Furthermore, conventional QDs are characterized by a small Stokes shift (energy separation between QD absorption onset and QD emission) and, thereby, substantial self-reabsorption, a principal limitation for phosphor applications[4] due to resulting dramatic losses in down-conversion efficiency.[13,14]

We have previously described a core/thick-shell QD architecture—the so-called "giant" QD (gQD)—for which many of the deleterious "dark" processes are suppressed and self-reabsorption is minimized by the physical and energetic separation of the processes of absorption and emission, i.e., the thick shell (comprising >90% of the total particle volume) is the principal absorber and the core the sole emitter.[13,15−17] We have explored this latter attribute of gQDs before.[13] Here, we elucidate two further aspects of gQD emitters as down-conversion phosphors: (1) retention of solution-phase QY in the solid-state and the resulting possibility for near-unity (>85%) down-conversion efficiencies, and (2) response to varying photon flux, including significantly enhanced efficiency and stability under high photon-flux (obtained at high driving currents: >200 mA) compared to standard core/shell QDs.

Solid-state down-conversion efficiencies were determined for both CdSe/CdS gQDs and standard CdSe/CdS core/thin-shell QDs (Figure 1). In all cases, the gQD shells comprised at least 10 CdS monolayers (one monolayer, ML, equals 0.3375 nm), which amounted to a shell-to-core volume ratio of at least 95:1. The gQD samples were chosen to represent a range of solution-phase QYs from 20 to 89%. The thin-shell CdSe/CdS sample employed here possessed an intermediate QY of 40%, and the shell layer was made up of 3 ML CdS. In this case, the shell is still the primary contributor to total particle volume (~70%), but as we show below self-reabsorption nevertheless limits down-conversion efficiencies in the solid-state.

To construct the device, a thin slab of gQD or QD-polymer composite was adhered directly to a blue LED (similar to Figure 1a inset but without an intervening spacer layer; see below). Poly(lauryl methacrylate) (PLMA) was chosen as the polymer matrix due to its chemical compatibility with the gQD/QD surface ligands, i.e., the 13-carbon-long alkyl side chain of PLMA can interpenetrate the alkyl substituents of the oleate [9-carbon alkyl substituents: $CH_3(CH_2)_7CH{=}CH(CH_2)_7COO^-$] or oleylamine [9-carbon alkyl substituents $CH_3(CH_2)_7CH{=}CH(CH_2)_7CH_2NH_2$] gQD/QD surface ligands and afford stabilizing interactions that limit disruption of the QD-binding head groups (carboxylate or amine, respectively). In principle, use of PLMA should limit the emission efficiency losses that otherwise result from damage to the ligand shell during the transition from the solution-phase to the solid state.[18] A Philips Lumileds high power "royal blue" Luxeon Rebel ES LED was used as the excitation source, as it allowed operation over a wide range of operating currents (0−500 mA). All measurements to assess light output and resulting down-conversion efficiency were conducted in an integrating sphere to ensure quantitative collection of source and down-converted photons (see the Supporting Information). Finally, we note that the small particle sizes characteristic of these emitters (gQD diameters: ~10−20 nm; QD diameters: <6 nm) afford optically clear films that are not compromised by particle-induced scattering losses.

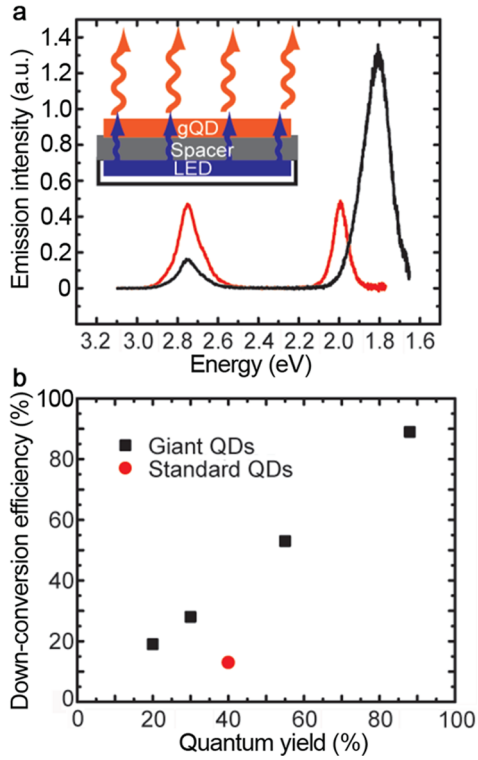

Figure 1. (a) Remnant blue-LED electroluminescence (2.76 eV; 450 nm; 200 mA driving current) and red (<2.0 eV; >600 nm) gQD (black trace) or QD (red trace) photoluminescence. Inset: device schematic; "spacer layer" is either absent (phosphor deposited directly onto the LED surface) or comprises PDMS, silica aerogel, or air. (b) Solid-state down-conversion efficiency as a function of gQD or QD solution-phase QY (200 mA driving current in all cases).

Blue LED electroluminescence (EL) and red gQD or QD PL spectra for both gQD and QD devices are shown in Figure 1a. Identical QD masses were used to prepare the polymer composite films for each device [2 mg in 6 mL LMA monomer preparation (see the Supporting Information for details), resulting in an optical density at 450 nm for ~2−2.5 mm thick films of 2.3 for gQDs and 1.5 for QDs], and each was driven by a 200 mA current. gQD (12 ML CdS shell) solution-phase QY was 30%, whereas that for the QDs (3 ML CdS shell) was 40%. Despite the higher solution-phase QY, the thin-shell CdSe/CdS QDs were comparatively poorer down-converters in the solid-state. As shown in Figure 1b, this gQD-polymer layer down-converted ~30% of the LED-source photons, whereas the QD-polymer layer successfully converted only 13% of blue photons to red photons (values determined by comparing integrated intensities for the blue EL before the emitter layers are added with that for the gQD/QD red PL; see the Supporting Information, Table S1).

DOI: 10.1021/acsami.5b02818
ACS Appl. Mater. Interfaces 2015, 7, 13125−13130

The relatively poor performance of standard core/shell QDs results in large part from detrimental self-reabsorption caused by the characteristic small QD Stokes shift (~10−15 nm separation between PL peak and absorption onset). Though largely absent in the relatively dilute solution-phase, this effect manifests in concentrated solid-state films. Furthermore, standard QDs are poorer absorbers. Namely, absorption cross sections for CdSe/CdS QDs as a function of shell thickness have been determined,[19] and the cross-section for a CdSe/CdS gQD comprising 12 MLs of CdS is ~12 times that for the 3 ML thin-shell QD. For this reason, fewer blue photons are absorbed by the QD/PLMA layer as evident in a more intense remnant blue EL (Figure 1a). Specifically, the gQD film absorbed almost 100% of the blue EL, leaving only 1−2% unabsorbed, whereas the same mass of QDs left 12% unabsorbed blue photons. Thus, approximately 6−12 times fewer blue photons were absorbed by the QD layer compared to the gQD layer, which is similar to the difference between respective absorption cross sections. Nevertheless, if photon absorption were the only challenge facing QD devices, down-conversion efficiency for a 40% QY phosphor should reach close to 30% for the mass of QDs employed here. Since it does not, we suggest that photon conversion is compromised in these materials, again, likely due primarily to self-reabsorption.[13,20] Importantly, although increasing the QD content in the QD/PLMA absorber layer would result in enhanced absorption of LED source photons, possible benefit to overall down-conversion efficiency would be negated by additional self-reabsorption.[13]

The new ability of gQDs to afford solid-state down-conversion efficiencies that fully track with their solution-phase QYs was further demonstrated for the range of QYs from 20 to 89% (Figure 1b and Table S1 in the Supporting Information; corresponding to different gQD preparations for which QY varied). Although high solid-state QYs have been observed previously (to 40−45%),[18,21] reported LED down-conversion efficiencies are significantly lower. Our prior work was limited by the starting solution-phase QY and suboptimal device design to a down-conversion efficiency of <25%,[13] whereas others observed dependencies on QD/polymer layer thickness, such that the best result (~11% down-conversion) was obtained for the thinnest film, with thicker emitter layers dropping to ~1% efficiency. In that case, poor down-conversion was attributed to self-reabsorption processes as well as insufficient penetration of blue light into the thicker layers and possible increased scattering of red light.[22] Here, we show the possibility to approach 100% down-conversion efficiency with an "on-chip" phosphor configuration that is only limited by the QY of the phosphor material and, as we discuss below, effects of high driving current and/or temperature.

Thermal quenching of QD PL is a well-known, if not fully understood, phenomenon.[23,24] This quenching, which results from increasing temperature, may or may not be accompanied by changes in PL lifetimes: "dynamic" vs "static" quenching, respectively. We have shown previously that nonemissive or "dark" processes leading to another well-known phenomenon of QD photophysics, blinking, can also be either dynamic or static in nature.[25] Namely, the blinking mechanism referred to as "A-type" entails intensity reductions accompanied by PL lifetime shortening, whereas "B-type" photodarkening occurs in the absence of lifetime changes and appears to result from "hot" electron capture to surface trap states[25] or hole capture to deep traps also associated with the QD surface or other defect sites.[26] While we do not attempt a complete inquiry into gQD thermal quenching in this study, we do observe several features of gQD thermal response germane to applications in white-light LEDs. Namely, thermal quenching from room-temperature to ~100 °C is reversible (Figure 2a) and accompanied by a less than 10

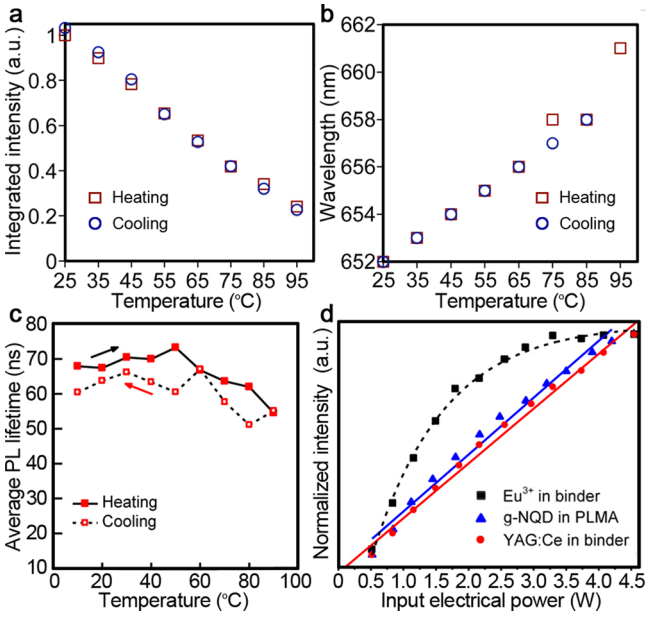

Figure 2. (a, b) Photoluminescence intensity of a representative gQD/PLMA composite as a function of temperature reveals linear and reversible thermal quenching and red-shifting, respectively. (c) Impact of temperature on gQD average PL lifetime. (d) Normalized PL intensity as a function of photon flux compared for three phosphor materials: Eu(III) nitrate salt and Ce(III)-doped $Y_3Al_5O_{12}$ (YAG:Ce) in gamma-butyrolactone (binder) and gQDs in PLMA. (Note: lines through data are simply guides to the eye and each data set is normalized to the maximum brightness.).

nm (equally reversible) red-shift (Figure 2b). Furthermore, the observed quenching is "static", at least to ~85 °C (Figure 2c), possibly implying a mechanistic relationship to B-type blinking. It is perhaps curious that although B-type blinking is suppressed in gQDs, these otherwise photostable emitters still exhibit reversible thermal quenching. We note that two processes may be responsible for this apparent contradiction, thermally activated carrier escape to pre-existing trap states and/or thermally activated temporary trap-state formation,[23] which could allow B-type carrier capture to "reappear" at elevated temperatures.

In addition to thermal quenching, down-converter materials in SSL may also suffer from flux saturation, whereby the emitter does not convert all available blue photons due to an inadequate "photon-cycling rate." This is the case for many rare-earth phosphors for which fluorescence decay is slow (microsecond decay times). For these phosphors, high-power sources can create a second excitation (or more) in an emitter already in an excited state. Visible-emitting QDs and gQDs possess relatively fast PL decay times (10−100s ns time scale) and for this reason are generally considered resistant to flux saturation. We show in Figure 2d flux-dependent PL intensities for the CdSe/CdS gQD, a fast-response rare-earth phosphor (Ce^{3+}:YAG in binder, gamma-butyrolactone) and a slow-response Eu^{3+} emitter (Eu^{3+} nitrate in same binder). In this case, the LEDs were clamped 6 mm away (air "spacer") from the phosphor films, and PL was measured on a spectroradi-

DOI: 10.1021/acsami.5b02818
ACS Appl. Mater. Interfaces 2015, 7, 13125−13130

ometer (see the Supporting Information for details). Although the former two respond linearly to increasing flux, the Eu^{3+} emitter exhibits flux saturation.

However, under ultrahigh fluxes (power densities ~5−10 W/mm^2), the average exciton population in gQDs can exceed one electron−hole pair due to factors other than PL decay rate. Specifically, in the case of gQDs synthesized with 12−15 monolayers of shell (i.e., for which absorption cross-section is very large: 100−300 × 10^{-15} cm^2),[19] we find that the average exciton population (which depends on excitation rate, cross-section, photon energy and decay lifetime; see the Supporting Information for detailed calculation) would range from ~3−60, clearly in the multiexciton regime. For lower but still high-flux operation (power density of 1 W/mm^2), average exciton population drops below 1 (i.e., on average the gQDs are excited with less than one electron−hole pair). Significantly, radiative recombination from the multiexciton states is precluded in conventional QDs because of very efficient nonradiative Auger recombination.[27,28] In contrast, since Auger recombination is suppressed in gQDs, biexciton and multiexciton emission is efficient, even at room temperature.[22] Thus, although the large absorption cross sections of gQDs cause their transition to multiexciton regimes under ultrahigh-flux operation, they are well-suited to such applications because of their unique (compared to standard QDs) ability to remain emissive under such conditions.

To assess the effects of photon flux and induced heating (see below) on phosphor performance in a more relevant device configuration, we tested a series of LEDs as a function of LED driving current from 50 to 500 mA (Figure 3a; note: currents were increased approximately every 3 min, allowing sufficient time for the emitter layer to achieve thermal equilibrium). The QD or gQD/PLMA films were either deposited directly onto the LED chip or onto a thin spacer layer as shown in Figure 1a inset; 2 mm polydimethylsiloxane (PDMS; a simple silicone polymer) or 2 mm silica aerogel spacers were employed. The purpose of the spacer was to minimize conductive heating at the phosphor layer caused by LED junction heating (Figure S1 in the Supporting Information). Its presence should not influence heating caused by the Stokes-shift loss mechanism (process of higher energy "blue" LED photons being converted to lower energy "red" re-emitted photons produces heat) or the QY-loss mechanism (photons that are absorbed but not re-emitted due to <100% QY are converted to heat). PDMS was chosen because of its compatibility with standard silicone chemistry used currently by the lighting industry, while aerogel was investigated as a novel material with exceptionally low thermal conductivity (~5 mW m^{-1} K^{-1}).[29] We find that at 200 mA or below gQD devices without a spacer layer afford the highest output intensities. Although falling short of a linear increase with increasing flux (approximate linear trajectory visualized by continuing a line connecting intensities for 50 and 100 mA driving currents), direct-on-chip gQD PL intensities are enhanced in the range from 100 to 200 mA and are quantitatively brighter than gQD devices incorporating either type of spacer, as "spacer" devices are compromised by imperfect transmittance of the LED blue photons to the phosphor layer (PDMS layers lose photons through wave-guiding out the sides of the device, while aerogel layers scatter the blue LED light: see the Supporting Information, Figure S2). However, at 250 mA, the PL intensities for both the direct-on-chip and the PDMS-spacer devices drop below their respective maximum intensities (achieved at 200 mA), while the aerogel-spacer device retains its maximum intensity to 400 mA. At 400 mA and above, both spacer-incorporated devices outperform the direct-on-chip device, with the aerogel spacer affording the highest absolute intensity from 350 to 500 mA. We surmise that this is due to the aerogel's ability to afford the best protection against thermal quenching resulting from conductive heating, suggesting that this source of "thermal load" plays an important role in determining phosphor performance in devices run at high currents. Notably, despite a similar solution-phase QY compared to the gQDs (40% vs 30%), the QD direct-on-chip device quickly succumbs to thermal quenching and/or flux-enhanced degradative quenching, yielding intensities substantially lower than any gQD device.

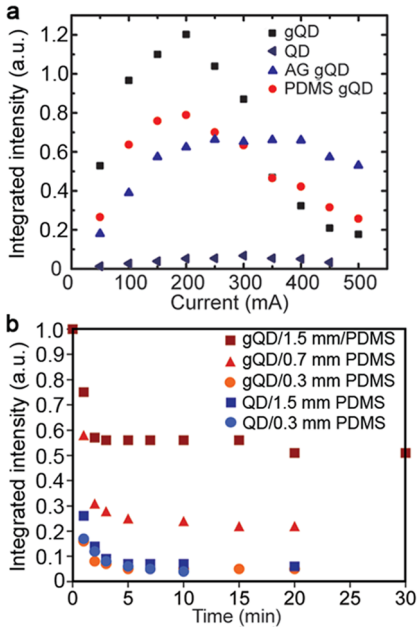

Figure 3. (a) Red PL intensity as a function of current for gQD or QD emitters and different spacer layers: no spacer, aerogel (AG), and silicone polymer (PDMS). (b) Temporal stability of different devices operated at 500 mA as a function of emitter (gQD or QD) and device architecture (PDMS spacer layer thickness).

PL intensity stability over time for gQD or QD emitters coupled to the high-power blue LED operated at a driving current of 500 mA was assessed for a series of device architectures (Figure 3b) − no spacer and PDMS spacers from 0.3 to 1.5 mm in thickness. Silicone PDMS spacers were used for this series due to their potential compatibility with existing lighting technologies. An attempt was made to collect PL spectra immediately following activation of the devices. However, we observed that for the gQD devices fabricated using thinner PDMS spacers and both QD devices the peak "instant on" intensity was likely not captured because of rapid quenching. Thus, the "zero time" point is only shown for the gQD device prepared using the thickest spacer (1.5 mm PDMS). Interestingly, in all cases, after initial quenching an approximately "steady state" intensity is reached that is maintained for the duration of the experiment (20 or 30 min). gQD intensity levels showed a strong correlation with PDMS layer thickness, with the thicker layers affording enhanced protection under the high flux operation (Figure 3b; note: the opposite intensity trend is observed in the case of lower driving currents, for which thermal "protection" is not

DOI: 10.1021/acsami.5b02818
ACS Appl. Mater. Interfaces 2015, 7, 13125−13130

required, such that gQD intensity is highest for thinner spacers that more effectively transmit LED photons to the emitter layer. The reversal of this trend at high currents further underscores the significance of the spacer in limiting conductive heating). In contrast, QD devices nearly completely quench regardless of layer thickness (1.5 or 0.3 mm PDMS).

Comparing the initial PL intensity obtained for the gQD/1.5 mm-spacer device with its steady-state level, we observe that ∼55% of the instant-on intensity is retained. Using the intensity−temperature correlation curve in Figure 2a, we infer that this gQD layer is operating at ∼65 °C − assuming all quenching is due to thermal quenching effects. However, if in addition to intensity quenching, one considers the extent of PL red-shifting, it becomes apparent that additional factors are likely at play. Namely, heating to ∼100 °C causes a PL red shift that is <10 nm (Figure 2b), but operation at 500 mA leads to a larger peak shift of 25−30 nm (see the Supporting Information, Table S2). The excessive red-shifting compared to that anticipated from heating alone could be an indicator that other processes contribute to the observed PL quenching. Energy transfer (ET) and self-reabsorption are processes that could lead to preferential emission from lower-energy gQDs in the ensemble of emitters, i.e., ET entails relatively higher energy ("bluer") gQDs in the ensemble transferring excitons to relatively lower energy ("redder") gQDs by way of nonradiative dipole−dipole interactions, whereas self-reabsorption involves the absorption of relatively bluer photons by other gQDs in the ensemble. Neither process, though, would be expected to yield red-shifting with a flux or driving-current dependency, which we further observe (see the Supporting Information, Table S2). Moreover, we have previously shown that the thick gQD shell causes strong suppression of both ET[20] and self-reabsorption[13] compared to conventional QDs. As PL intensity and peak position are equally important parameters to control in the context of general lighting applications, the observed unexpected nonthermally induced red-shifting is the subject of ongoing investigations. We hypothesize that much of the noted red-shifting and some of the observed PL quenching may arise from an electric field effect, induced by the collection of charge in the local environment of the emitters.[30] This effect would be expected to have a flux dependency as higher driving currents could lead to enhanced photocharging (by carrier trapping or ejection) of the gQDs (likewise for QDs), effecting a photoinduced change in the dielectric environment.

In summary, we have explored the potential of red-emitting QDs and gQDs for "on-chip" phosphor applications. Using the thick-shell gQDs, we show for the first time that semiconductor nanocrystal alternatives to rare-earth phosphors can provide near-unity down-conversion of blue LED light as a result of retained solution-phase QYs in the solid-state. However, direct-on-chip performance is compromised for both QD and gQD emitters by thermal quenching and, possibly, other flux-induced quenching mechanisms exacerbated by operation at high driving currents (>200 mA). Nevertheless, gQD PL in particular can be stabilized at significantly reduced quenching levels by incorporation of a thin spacer layer. The observation that incorporation of a thermal spacer substantially reduces quenching suggests that conductive heating is an important parameter to be considered in the design of next-generation "phosphor-on-chip" light-emitting devices. That said, we additionally observe that thermal quenching alone is not responsible for performance degradation, and we suggest that understanding photocharging processes may play a key role in optimizing efficiency and operational lifetime of QD-down-converted LEDs.

■ ASSOCIATED CONTENT

Supporting Information

Detailed materials and methods and additional figures. The Supporting Information is available free of charge on the ACS Publications website at DOI: 10.1021/acsami.5b02818.

■ AUTHOR INFORMATION

Corresponding Author

*E-mail: jenn@lanl.gov.

Notes

The authors declare no competing financial interest.

■ ACKNOWLEDGMENTS

Research supported primarily by a Single Investigator Small Group Research Grant (2009LANL1096), Division of Materials Science and Engineering (MSE), Office of Basic Energy Sciences (OBES), Office of Science (OS), U.S. Department of Energy (DOE), including funding for J.A.H., H.H., C.J.H., K.A., X.M., and S.B. The work was performed in large part at CINT. J.K. conducted some of the preliminary studies leading to this work, whereas J.A.T. and C.E.H. provided the aerogel films, and acknowledge Los Alamos National Laboratory (LANL) Directed Research and Development Funds. LANL, an affirmative action equal opportunity employer, is operated by Los Alamos National Security, LLC, for the National Nuclear Security Administration of the U.S. DOE under contract DE-AC52-06NA25396.

■ REFERENCES

(1) Navigant Consulting, Inc. *2010 U.S. Lighting Market Characterization*; U.S. Department of Energy: Washington, D.C., 2012.

(2) George, N. C.; Denault, K. A.; Seshadri, R. Phosphors for Solid-State White Lighting. *Annu. Rev. Mater. Res.* **2013**, *43*, 481−501.

(3) Phillips, J. M.; Coltrin, M. E.; Crawford, M. H.; Fischer, A. J.; Krames, M. R.; Mueller-Mach, R.; Mueller, G. O.; Ohno, Y.; Rohwer, L. E. S.; Simmons, J. A.; Tsao, J. Y. Research Challenges To Ultra-Efficient Inorganic Solid-State Lighting. *Laser Photonics Rev.* **2007**, *1*, 307−333.

(4) Wen, D.; Shi, J. A Novel Narrow-Line Red Emitting $Na_2Y_2B_2O_7$:Ce^{3+},Tb^{3+},Eu^{3+} Phosphor with High Efficiency Activated by Terbium Chain for Near-UV White LEDs. *Dalton Trans.* **2013**, *42*, 16621−16629.

(5) Lin, C. C.; Liu, R.-S. Advances in Phosphors for Light-Emitting Diodes. *J. Phys. Chem. Lett.* **2011**, *2*, 1268−1277.

(6) Shen, C.; Chu, J.; Qian, F.; Zou, X.; Zhong, C.; Li, K.; Jin, S. High Color Rendering Index White LED Based On Nano-YAG:Ce^{3+} Phosphor Hybrid With CdSe/CdS/ZnS Core/Shell/Shell Quantum Dots. *J. Mod. Opt.* **2012**, *59*, 1199−1203.

(7) Hu, Y.; Zhuang, W.; He, H.; Liu, R.; Chen, G.; Liu, Y.; Huang, X. High Temperature Stability Of Eu^{2+}-Activated Nitride Red Phosphors. *J. Rare Earths* **2014**, *32*, 12−16.

(8) Ziegler, L.; Xu, S.; Kucur, E.; Meister, F.; Batentschuk; Gindele, F.; Nann, T. Silica-Coated InP/ZnS Nanocrystals as Converter Material in White LEDs. *Adv. Mater.* **2008**, *20*, 4068−4073.

(9) Aboulaich, A.; Michalska, M.; Schneider, R.; Potdevin, A.; Deschamps, J.; Deloncle, R.; Chadeyron, G.; Mahiou, R. Ce-Doped YAG Nanophosphor and Red Emitting $CuInS_2$/ZnS Core/Shell Quantum Dots for Warm White Light-Emitting Diode with High Color Rendering Index. *ACS Appl. Mater. Interfaces* **2013**, *6*, 252−258.

(10) Qu, L.; Peng, X. Control of Photoluminescence Properties of CdSe Nanocrystals in Growth. *J. Am. Chem. Soc.* **2002**, *124*, 2049−2055.

DOI: 10.1021/acsami.5b02818
ACS Appl. Mater. Interfaces 2015, 7, 13125−13130

(11) Greytak, A. B.; Allen, P. M.; Liu, W.; Zhao, J.; Young, E. R.; Popović, Z.; Walker, B. J.; Nocera, D. G.; Bawendi, M. G. Alternating Layer Addition Approach to CdSe/CdS Core/shell Quantum Dots with Near-Unity Quantum Yield and High On-Time Fractions. *Chem. Sci.* **2012**, *3*, 2028−2034.
(12) Klar, T. A.; Franzl, T.; Rogach, A. L.; Feldmann, J. Super-Efficient Exciton Funneling in Layer-by-Layer Semiconductor Nanocrystal Structures. *Adv. Mater.* **2005**, *17*, 769−773.
(13) Kundu, J.; Ghosh, Y.; Dennis, A. M.; Htoon, H.; Hollingsworth, J. A. Giant Nanocrystal Quantum Dots: Stable Down-Conversion Phosphors that Exploit a Large Stokes Shift and Efficient Shell-to-Core Energy Relaxation. *Nano Lett.* **2012**, *12*, 3031−3037.
(14) Mueller, G. O. In Color Conversion of LED Light. In *Phosphor Global Summit*; San Diego, CA, Feb 28−March 2, 2005 ; Intertech: St. Paul, MN, 2005; Vol. *11*, p 1.
(15) Chen, Y.; Vela, J.; Htoon, H.; Casson, J. L.; Werder, D. J.; Bussian, D. A.; Klimov, V. I.; Hollingsworth, J. A. Giant" Multishell CdSe Nanocrystal Quantum Dots with Suppressed Blinking. *J. Am. Chem. Soc.* **2008**, *130*, 5026−5027.
(16) Ghosh, Y.; Mangum, B. D.; Casson, J. L.; Williams, D. J.; Htoon, H.; Hollingsworth, J. A. New Insights into the Complexities of Shell Growth and the Strong Influence of Particle Volume in Non-Blinking "Giant" Core/Shell Nanocrystal Quantum Dots. *J. Am. Chem. Soc.* **2012**, *134*, 9634−9643.
(17) Dennis, A. M.; Mangum, B.; Piryatinski, A.; Park, Y.-S.; Hannah, D.; Casson, J.; Williams, D.; Schaller, R.; Htoon, H.; Hollingsworth, J. A. Suppressed Blinking and Auger Recombination in Near-Infrared Type-II InP/CdS Nanocrystal Quantum Dots. *Nano Lett.* **2012**, *12*, 5545−5551.
(18) Lee, J.; Sundar, V. C.; Heine, J. R.; Bawendi, M. G.; Jensen, K. F. Full Color Emission from II−VI Semiconductor Quantum Dot−Polymer Composites. *Adv. Mater.* **2000**, *12*, 1102−1105.
(19) Park, Y.-S.; Malko, A. V.; Vela, J.; Chen, Y.; Ghosh, Y.; García-Santamaría, F.; Hollingsworth, J. A.; Klimov, V. I.; Htoon, H. Near-Unity Quantum Yields of Biexciton Emission from CdSe/CdS Nanocrystals Measured Using Single-Particle Spectroscopy. *Phys. Rev. Lett.* **2011**, *106*, 187401.
(20) Pal, B. N.; Ghosh, Y.; Brovelli, S.; Laocharoensuk, R.; Klimov, V. I.; Hollingsworth, J. A.; Htoon, H. Giant" CdSe/CdS Core/Shell Nanocrystal Quantum Dots As Efficient Electroluminescent Materials: Strong Influence of Shell Thickness on Light-Emitting Diode Performance. *Nano Lett.* **2012**, *12*, 331−336.
(21) Meinardi, F.; Colombo, A.; Velizhanin, K. A.; Simonutti, R.; Lorenzon, M.; Beverina, L.; Viswanatha, R.; Klimov, V. I.; Brovelli, S. Large-area Luminescent Solar Concentrators Based on 'Stokes-Shift-Engineered' Nanocrystals in a Mass-Polymerized PMMA Matrix. *Nat. Photonics* **2014**, *8*, 392−399.
(22) Wood, V.; Panzer, M. J.; Chen, J.; Bradley, M. S.; Halpert, J. E.; Bawendi, M. G.; Bulović, V. Inkjet-Printed Quantum Dot−Polymer Composites for Full-Color AC-Driven Displays. *Adv. Mater.* **2009**, *21*, 2151−2155.
(23) Zhao, Y.; Riemersma, C.; Pietra, F.; Koole, R.; de Mello Donegá, C.; Meijerink, A. High-Temperature Luminescence Quenching of Colloidal Quantum Dots. *ACS Nano* **2012**, *6*, 9058−9067.
(24) Rowland, C. E.; Schaller, R. D. Exciton Fate in Semiconductor Nanocrystals at Elevated Temperatures: Hole Trapping Outcompetes Exciton Deactivation. *J. Phys. Chem. C* **2013**, *117*, 17337−17343.
(25) Galland, C.; Ghosh, Y.; Steinbrück, A.; Sykora, M.; Hollingsworth, J. A.; Klimov, V. I.; Htoon, H. Two Types of Luminescence Blinking Revealed by Spectroelectrochemistry of Single Quantum Dots. *Nature* **2011**, *479*, 203−207.
(26) Qin, W.; Guyot-Sionnest, P. Evidence for the Role of Holes in Blinking: Negative and Oxidized CdSe/CdS Dots. *ACS Nano* **2012**, *6*, 9125−9132.
(27) Caruge, J.-M.; Chan, Y.; Sundar, V.; Eisler, H. J.; Bawendi, M. G. Transient Photoluminescence and Simultaneous Amplified Spontaneous Emission from Multiexciton States in CdSe Quantum Dots. *Phys. Rev. B* **2004**, *70*, 085316.
(28) Dang, C.; Lee, J.; Breen, C.; Steckel, J. S.; Coe-Sullivan, S.; Nurmikko, A. Red, Green and Blue Lasing Enabled by Single-Exciton Gain in Colloidal Quantum Dot Films. *Nat. Nanotechnol.* **2012**, *7*, 335−339.
(29) Li, L.; Yalcin, B.; Nguyen, B. N.; Meador, M. B.; Cakmak, M. Flexible Nanofiber-Reinforced Aerogel (Xerogel) Synthesis, Manufacture, and Characterization. *ACS Appl. Mater. Interfaces* **2009**, *1*, 2491−2501.
(30) Ioannou-Sougleridis, V.; Kamenev, B.; Kouvatsos, D. N.; Nassiopoulou, A. G. Influence of a High Electric Field on the Photoluminescence from Silicon Nanocrystals in SiO_2. *Mater. Sci. Eng.* **2003**, *B101*, 324−328.

DOI: 10.1021/acsami.5b02818
ACS Appl. Mater. Interfaces 2015, 7, 13125−13130